Understanding the relationship between biomass production and water use of Populus tomentosa trees throughout an entire short-rotation

Article

Accepted Version

Understanding the relationship between tree production and water use under changing environmental conditions in a short-rotation *Populus tomentosa* plantation

Doudou Li[1], Jinqiang Liu[1], Anne Verhoef[2], Benye Xi[1*], Virginia Hernandez-Santana[3*]

[1]Ministry of Education Key Laboratory of Silviculture and Conservation, Beijing Forestry University, Beijing, China

[2]Department of Geography and Environmental Science, The University of Reading, PO Box 227, Reading, RG6 6AB, United Kingdom

[3]Irrigation and Crop Ecophysiology Group, Instituto de Recursos Naturales y Agrobiología de Sevilla (IRNAS, CSIC), Avenida Reina Mercedes, nº. 10, 41012 Sevilla, Spain

Corresponding author:

Benye Xi (benyexi@bjfu.edu.cn); Virginia Hernandez-Santana (virginiahsa@gmail.com)

Ministry of Education Key Laboratory of Silviculture and Conservation, Beijing Forestry University, 35 East Qinghua Road, Beijing 100083, China

Phone number: +86 18638539681

Fax: +86 10 62337055

Abstract

Understanding the relationship between tree production and water use, as well as the main environmental and plant-related drivers of water use, is crucial for the establishment of production prediction models and reliable water management under current and future climatic conditions. However, the relation between tree water use and biomass production has never been assessed throughout the entire life-cycle of a poplar rotation; nor have detailed investigations been reported on how poplar transpiration and its regulation change inter-annually. Therefore, we studied the relationship between transpiration (*E*) and aboveground biomass (ABM), as well as the main drivers of *E*, in a plantation established on the North China Plain, with 2- to 5-year-old (2016 to 2019) *Populus tomentosa* trees under three water treatments. Our results indicated that ABM increase depended on annually accumulated *E* and that their relationship can be fitted with a logistic curve for the entire life cycle ($R^2 >$ 0.89). Throughout the whole rotation period, compared with non-irrigated trees, full irrigation trees produced 59% more biomass with only 12% more *E*, while deficit irrigation trees attained 46% more biomass with 32% more *E*. The daily *E* had a strong exponential relationship with vapor pressure deficit (*D*) during years 3-5 of their growth cycle, which the asymptote of this relationship increasing with tree age (1.6 kPa (2017), 2 kPa (2018), 2.5 kPa (2019)). The *E* was also strongly linearly correlated to solar radiation (R_s) for each year although with slightly weaker relationships than for *D*. Similar to other poplar clones, *P. tomentosa* showed effective stomatal control on *E*. However, soil water content had almost no effect, for all treatments, no matter which soil layer was considered. Finally, our research quantified the relationship between tree production and water use throughout the rotation. We also confirmed that *D* and R_s are indeed the major drivers of transpiration during the growing season as well as during drought in this semi-humid boreal region. Our findings should enable a better understanding of the water-use strategies of poplars in the North China Plain and will help sustainably manage plantations in water-scarce regions around the world under changing environmental conditions.

Key words

Sap flow; Yield; Environmental variables; Stomatal conductance; Drought; Poplar

1. Introduction

Poplar plantations are widely distributed around the world, with a total area of more than 31 million ha (FAO, 2016). According to the latest report by FAO (2016), Canada accounted for 21.8 million ha of planted poplar area (69% of the global area), China for 8.5 million (27% of the global area), followed by France with 0.2 million ha, and finally by Turkey, Iran, Spain and the USA (0.1 million ha each). *Populus tomentosa* is ubiquitous in poplar plantations on the North China Plain, planted over an area of > 340,000 ha (Zhang et al., 2012; Xi, 2013). In this region, seasonal drought occurs regularly, due to the nature of the monsoonal climate. Consequently, water is usually a crucial limiting factor for poplar growth due to the high-water utilization rates of this species (Xi et al., 2016; Di et al., 2019a). Climate change projections indicate reduced summer precipitation and increased air temperatures for the North China Plain (Kang and Eltahir, 2018). Thus, irrigation could become a necessary measure to enhance tree production in such plantations (Xi et al., 2016; Li et al., 2020). However, the relation between tree water use and biomass production has never been assessed thoroughly throughout the entire rotation of poplar. There are only two examples examining this relationship but none of them evaluated a full rotation. Orság and Trnka (2011) measured this relationship, but only for one month, while Fischer et al. (2014) researched this relationship for two growing seasons; both studies were for poplar clone J-105 (*P. nigra* × *P. maximowiczii*) and were conducted in the Czech-Moravian highlands. In both cases the relationship between water use and biomass production was positive and linear, although, according to Fischer et al. (2014), this relationship could change as the plantation matures, which could have important consequences for the irrigation management of the plantation.

Moreover, in addition to changes in the biomass-water use relationships caused by tree maturation, this relationship could also change as a function of environmental variables, as tree water use responds markedly to changes in soil water content (SWC), vapour pressure deficit (D) and solar radiation (R_s) (e.g. Hernández-Santana et al., 2008; Tognetti et al., 2009; Tie et al., 2017; Wang et al., 2017), largely as a result of regulation via stomatal conductance (Allen et al., 1999; Zhang et al., 1999; Larchevêque et al 2011). Specifically, Liang et al. (2006) found that soil water deficit severely limited the transpiration of *P. simonii* during dry seasons. Chen et al. (2014) reported that changes in D and R_s affected poplar transpiration on short timescales, while the effect of SWC became important on longer temporal scales. Other studies have shown that D fluctuation leads to the alteration of poplar transpiration rate (Franks et al. 2007) by affecting stomatal conductance (Meinzer et al. 1997; Kucerova

et al. 2010; Renninger et al. 2010). However, Larchevêque et al. (2011) and Hamanishi et al. (2010) found some variability in the type and degree of stomatal control among poplar species and clones. Other studies suggested that the impact of each environmental variable on tree transpiration varied with climatic region, species and tree age (Oogathoo et al., 2020). To our knowledge, no attempt has been made to investigate how tree transpiration and its regulation changes interannually for *P. tomentosa* in response to varying environmental conditions. Therefore, in order to design management strategies that minimize the use of irrigation water, it is necessary to develop a thorough understanding of the effects of environmental drivers on the water use of poplar plantations along a whole rotation.

Therefore, the objectives of this study are (1) to quantify the relationship between transpiration and biomass and (2) identify the main environmental and plant controls on water use of *P. tomentosa* during a whole short rotation under different soil water supply conditions. Accurate assessment of the relationship between poplar water use and biomass will help improve irrigation scheduling, e.g., for sub-humid areas like the North China Plain. To fulfill these objectives, we measured transpiration, tree biomass, key environmental variables (D, R_s and SWC) and stomatal conductance in *P. tomentosa* plantations under three irrigation treatments (including rainfed) during years 2-5 of one short rotation (from 2016 to 2019). We hypothesize that (1) the relationship between accumulated transpiration and biomass production of *P. tomentosa* is strongly positive and linear, and that this relationship changes for different tree ages and different water supply conditions, along the entire rotation period. We also hypothesize that (2) D and R_s are the main drivers of transpiration during the growing season for trees under sufficient water supply, (3) but that under water deficit conditions tree water use depends mainly on soil water content.

2. Materials and Methods

2.1. Experimental site and treatments

The study was conducted at the state-owned Jiucheng Forest Farm, in Gaotang County, Shandong Province (latitude: 36.81°N, longitude: 116.09 °E, elevation: 30 m) from 2016 to 2019. The farm is situated in a typical Yellow River alluvial plain located in northern China. The climate in the region is warm temperate monsoon, with average air temperature of 13.41 ℃ and average annual rainfall of 562.9 mm (1981–2010 period). The experimental site is flat and has relatively stable groundwater levels, located at about 6–9 m depth. The soil layers between 0–1.4 m have a sandy loam texture (sand : silt :

clay is 62.9% : 34.6% : 2.5%), whereas between 1.4–3.0 m there is silt loam (sand : silt : clay is 29.6% : 65.5% : 4.9%). The soil in the 0.0–0.4 m layer has a pH of 8.1, available N of 41.5 mg kg^{-1}, available P of 7.11 mg kg^{-1}, 76.8 mg kg^{-1} available K and 0.94% organic matter.

The experimental plantation was established in April 2015 with the clone B301 ((*P. tomentosa* × *P. bolleana*) × *P. tomentosa*) of *P. tomentosa*. The trees were spaced 2 m apart within the tree row and 3 m between rows, leading to a tree density of 1666 trees ha^{-1}. On average, the height and diameter at breast height (DBH) of trees were 3.0±0.1 m and 3.7 ±0.2 cm, respectively, in April 2016, at the beginning of the experiments. Three soil water treatments were implemented: drip full irrigation treatment (DIFI), drip deficit irrigation treatment (DICI) and one non-irrigation treatment (CK). Each year, in order to encourage the leaf out, one irrigation (i.e., leaf spreading irrigation) was applied for all treatments at the time of tree budding around early April, after which the three water treatments started. In 2016 and 2017, further irrigation was initiated when the average soil matric potential at 0.2 m depth below the drippers reached -20 kPa and -45 kPa for DIFI and DICI treatments, respectively. In 2018 and 2019, the original irrigation threshold for DIFI treatment was increased to -18 kPa while the threshold for the DICI treatment was left unchanged. The irrigation period lasted from April to October, with further details given in Li et al. (2020). For each treatment, we had five 24 m × 18 m plots (i.e., five replicates), with 72 trees each (eight tree lines with nine trees per line), distributed in a completely randomized block design. Within each plot we considered the 20 central trees for measurements and left the others as border trees. Each tree was fertilized with 80 g N per year and herbicide was regularly applied for weed control. This experiment is part of a larger project with two further irrigation treatments.

2.2 Micrometeorological conditions

Measurements of air temperature (T_a, ℃), precipitation (P, mm day^{-1}), solar radiation (R_s, MJ m^{-2} day^{-1}) and relative humidity (RH, %) were obtained at a weather station (Delta-T Devices Ltd, Cambridge, UK) installed at a distance of 0.9 km from the experimental site. Air vapor pressure deficit (D, kPa) was derived from RH and T_a, using the empirical equation given in Campbell and Norman (1998). All variables were measured every 10 minutes from April to October between 2016 to 2019. Daily total P, total solar radiation R_s, and average D were calculated based on these records.

2.3 Soil water potential, soil water content monitoring and simulation

Soil matric potential (Ψ_m, kPa) measurements were made in the vicinity of five representative trees for both DIFI and DICI treatments, with all five growing in one single plot. For each of these five trees we installed one tensiometer (TS30, Shunlong, Beijing, China) at 0.2 m below a dripper to measure Ψ_m. Data were recorded manually at about 8:00 am, every day, along the four irrigation seasons between 2016–2019.

Soil water content (SWC, m^3 m^{-3}) was measured between 0 to 260 cm soil depth with measurement intervals of 10 or 20 cm; measurements took place every 5–10 days, from mid-April to early October 2016–2019, for all treatments. For each treatment, we selected three trees near which SWC profiles were measured. SWC was measured at a distance of 25, 50, 100 cm from each tree using a TDR probe (TRIME-IPH, IMKO Inc., Ettlingen, Germany).

In order to obtain a continuous set of daily SWC data, we used the HYDRUS-1D model to simulate the daily variation of SWC throughout the year. Optimized model parameters, such as saturated water content (θ_s, cm^3 cm^{-3}), residual water content (θ_r, cm^3 cm^{-3}), and saturated hydraulic conductivity (K_s, cm d^{-1}) were obtained through calibration with measured SWC data (R^2=0.90, Mean Weighted Absolute Error=0.02 cm^3 cm^{-3}, Root Mean Square Error=0.02 cm^3 cm^{-3}) (data not shown). We divided the profile of simulated daily SWC into four soil layers, informed by distinct differences in soil hydraulic parameters; hence, in our analyses we used the simulated daily average SWC of 0−40 cm ($SWC_{0\text{-}40}$), 50−80 cm ($SWC_{50\text{-}80}$), 90−160 cm ($SWC_{90\text{-}160}$) and 170−300 cm depths ($SWC_{170\text{-}300}$), respectively.

2.4 Transpiration estimates

Five representative sample trees per treatment, with initial average DBH of 4.25±0.16 cm in DIFI, 4.45±0.19 cm in DICI, and 4.48± 0.12 cm in CK, were selected in the same plot to measure trunk sap flux density (J_s, cm s^{-1}) from early April to the end of October, during all four years. For each tree, one set of thermal dissipation probes (TDP30, Dynamax Inc., TX, USA) was inserted into the sapwood about 1.5m above the ground on the south face of the trunk using the method of Granier (1987). In early April of each year, TDP30 probes were reinstalled on different trees in order to avoid permanently damaging the trees. Waterproof sealant was placed around the probes to prevent water from entering, and reflective bubble wrap insulation was used to wrap the probes and the trunk to minimize thermal gradients. Sap flux density was automatically measured every 10 s, and averages were calculated every 10 min and stored in a data logger (CR1000, Campbell Scientific Inc., North Logan, USA). These data

were used to estimate J_s according to Granier (1987), which was then converted to transpiration (E, mm d^{-1}) using the sapwood area at the sap flux measurement position. The sapwood area (SA, cm^2) was calculated using a relationship ($SA = 0.7587 \times DBH^{1.9541}$, $R^2 = 0.99$, n=202, $p < 0.0001$) between diameter and sapwood area measured on 100 harvest trees (see Section 2.6). For all the harvested trees, we measured DBH, bark thickness and pith diameter at different heights. SA was estimated as the part of the wood without bark and pith.

2.5 Stomatal conductance

In 2018, for each treatment, stomatal conductance (g_s) was measured using a leaf porometer (SC-1, Decagon Devices, Inc, USA) for three leaves on one tree used for sap flow measurements. The fully developed leaves were chosen at the east side of the canopy exposed to sunlight, approximately 5 m above the ground. Diurnal g_s values were measured half-hourly, from 8:00 am to 18:00 pm, on six sunny days (April 15th, April 18th, April 25th, May 13th, May 23th and June 20th). We also measured noon-time (around 11:30 am) g_s on a total of 50 sunny days from April 15th to September 3rd. In order to obtain continuous g_s values throughout the growing season, we established a relationship between g_s and J_s/D according to the method of Hernandez-Santana et al. (2016). Optimized model parameters were obtained through calibration with measured g_s at noon, for 50 sunny days (R^2=0.60, P<0.0001) (data not shown). Using this linear relationship, we were able to estimate g_s for every 10 minute interval, employing the continuously monitored data of J_s and D. From the simulated g_s data that were now available throughout the growing season, we calculated the maximum daily stomatal conductance (g_{smax}).

2.6 Stem growth and biomass

DBH was measured by a caliper with accuracy of 0.1 mm for all sap flow measurement trees, either monthly or bi-weekly from April to October during all four years.

Whole-tree harvests were conducted in June, September and November of 2016; June and September of 2017; October of 2018 and October of 2019. A total of 100 sample trees were selected to establish the relationship between DBH and biomass. For each of the six harvest seasons from 2016 to 2018, fifteen trees were selected for all five treatments belonging to the larger project from three randomly selected blocks. For the last harvest season of 2019, 10 trees were selected in the DIFI and CK treatments in a total of 5 blocks, respectively. Aboveground biomass was separated into branch and

stem fractions for each sample tree. Fresh mass of all tissues were weighed in the field, and representative subsamples were taken to the laboratory to determine their water content. All tissues were dried to constant mass at 70 °C before being weighed again. Dry biomass of wood was the dry biomass of branch + stem. Based on the biomass and DBH data of all 100 trees, we got the relationship between DBH and aboveground biomass (ABM, kg): $\mathrm{ABM} = 0.0319 \times DBH^{2.8303}$ (R^2 = 0.95, n=100, P < 0.0001). We used this equation to calculate the biomass of the trees instrumented.

2.7 Post-processing and statistical analyses

A total of fifteen trees in every growing season with 5 trees per treatment were used for the sap flow analyses. Based on the seasonal rainfall in the North China Plain, we divided our data into dry season (April to mid-June and early September to late October) and wet season (mid-June to late August), each year, to allow us to assess the effect of drought on the measured variables. Relative importance metrics of environmental predictors of tree sap flow were calculated using the R-package relaimpo (Grömping, 2006). The use of relative importance is appropriate when some of the regressors in a model are correlated (i.e., D and R_s), which is the case with our data. We calculated relative importance using the LMG (Lindeman, Merenda and Gold) method. LMG calculates the R^2 contribution averaged over orderings among regressors. All metrics were performed using the statistical software R (R Development Core Team, 2017).

For each year, logistic regressions were used to establish the relationship between accumulated E and ABM increase, linear relationships were used to describe the relationship between E and R_s, and exponential functions were used to describe the relationship between E and D. Decreasing exponential functions were used to describe how g_s and g_{smax} were regulated by D. In addition, in order to eliminate the effect of canopy development on tree water use, each meteorological factor was multiplied by leaf area index (LAI) before investigating the correlations between meteorological drivers and tree water use (Di et al., 2019 b). LAI was measured in 5 blocks for each treatment about every 15 days, the details of which can be found in Li et al. (2020). All figures were prepared using Origin 9.0 (OriginLab, USA).

3. Results

3.1 Micrometeorological and soil moisture conditions

Fig. 1 shows a summary of the meteorological variables throughout the 4 experimental years. Total P was 585 (2016), 449 (2017), 700 (2018), and 487 mm (2019), respectively, from April 1st to October

31th (Fig. 1a). Hence, 2018 was a distinctly different year, hydrologically speaking, that was much wetter than the other years. The first dry spring season normally runs from mid-April to mid-June, for which total *P* was 79 (2016), 85 (2017), 218 (2018), and 50 mm (2019). Hence, the 'dry' season in 2018 was in fact more representative of a wet season. The wet summer season generally falls between mid-June to early-September: total *P* for that period was 493 (2016), 295 (2017), 439 (2018), and 368 mm (2019). The dry autumn season usually occurs between the beginning of September and the end of October: total *P* was 47 (2016), 55 (2017), 35 (2018), and 45 mm (2019). With regards to global radiation: R_s for the dry spring season is larger than that for the wet summer season, as a result of higher cloud content during the rainy season (Fig. 1b). Average *D* is larger in the dry spring season than in the wet summer season, for 2016, 2017 and 2018, but not for 2019 (Fig. 1c). Both the average R_s and *D* were the lowest in the dry autumn season.

In the experimental plantation, the SWC of all soil layers was higher in the wet summer than in spring and autumn, except for $SWC_{50\text{-}80}$ in 2017. The SWC for the 0–40 cm soil layer displayed relatively high-frequency fluctuations, as a result of irrigation and rainfall inputs. SWC in this layer decreased in amount going from DIFI, DICI, to CK, in 2016, 2017 and 2019 (Fig. 1d). However, in 2018, $SWC_{0\text{-}40}$ was similar for all treatments, because of the higher rainfall in 2018. SWC in the 50–80 cm soil layer was similar among treatments in 2016 and during the spring dry season of 2017 (Fig. 1e). During the wet season (summer) of 2017 and 2019, $SWC_{50\text{-}80}$ for the DIFI treatment was larger than that of DICI, whereas the latter was approximately similar to that of CK. In 2018, $SWC_{50\text{-}80}$ was similar for all treatments. For the 90–160 cm soil layer (Fig. 1f), SWC differences among treatments were comparable with those found at 50–80 cm depth. Finally, for the deepest soil layer of 170–300 cm (Fig. 1g), the difference in SWC between DIFI and CK was bigger than for any of the other soil layers in 2019, with the range of $SWC_{170\text{-}300}$ for each treatment as follows: 0.28–0.41 (DIFI), 0.25–0.35 (DICI), and 0.16–0.30 (CK) $cm^3\ cm^{-3}$. Furthermore, even in the wet year of 2018, SWC of this soil layer was lower for CK than for DIFI and DICI treatments.

3.2 Relationship between transpiration and aboveground biomass

Fig. 2 shows that for each year and each treatment, ABM increase could be explained by the accumulated *E*, and their relationship was fitted with a separate logistic curve for each treatment (R^2 = 0.89–0.99, P<0.0001). This means that ABM first increased approximately in step with the accumulated *E*; then the ABM increase slowed down and ultimately stopped whereas *E* continued to accumulate for

a period of time. As the trees matured, the annually accumulated *E* gradually increased, from 150±20 mm year^{-1} (2016) to 723±157 mm year^{-1} (2019) (Fig. 2). Throughout the rotation, the annual ABM increase first increased and then decreased, reaching the largest values (14.1±2.3–17.7±0.9 kg/tree) in 2017 and the lowest (4.4±1.2 – 10.8±3.1 kg/tree) in 2019 (Fig. 2).

Compared with trees in the CK treatment (Fig 3), the percent increase (PI) of annual *E* was lower in DIFI than in DICI for each year. In contrast, the PI of annual ABM was higher in DIFI than in DICI from 2016 to 2018. During the whole rotation period, the PI of ABM was higher in DIFI (59%) than in DICI (46%) although it was lower in DIFI than in DICI in 2019. For the DIFI treatment, there was a lower *E* increment but a higher ABM increment for each year, compared with the CK treatment. The specific PI values of annual *E* & ABM in DIFI were -6% & 36% (2016), -9% & 32% (2017), 29% & 74% (2018) and 5% & 89% (2019). However, for the DICI treatment, the result was different, with higher PI for *E* than for ABM, from 2016 to 2017. In 2018 and 2019, the PI of ABM exceeded that of *E* in DICI. The negative PI values of annual *E* indicated the fact that DIFI trees consumed less water than CK trees in 2016 and 2017, which was possibly due to the transpiration compensatory effect of CK trees during the rainy season. This might be also the reason why the PI of annual *E* was lower in DIFI than in DICI for each year.

We also explored the relationship between total *E* and total ABM for the entire rotation period (Fig. 4), for each treatment. Total ABM increase could be explained by total *E,* and a logistic curve was fitted through the data (R^2 = 0.98–0.99, P<0.001). The shape and order of these curves was similar to the ones observed for biomass versus accumulated *E,* for each year separately. At the end of each growing season, the average total ABM of DIFI was always higher than that of DICI and CK, reaching 46.4 (DIFI), 41.7 (DICI) and 31.0 (CK) kg per tree in the final year. With regards to the average total *E* at the end of each growing season, values for DICI were always higher than those of DIFI and CK, leading to 1496.7 (DIFI), 1773.6 (DICI) and 1340.7 mm (CK) at the end of the last growing season. Over the whole rotation period, compared with CK, DIFI produced 59% more biomass with only 12% more *E*, while there was 46% more biomass, with 32% more *E*, for DICI.

3.3 Environmental and plant control of transpiration

Table 1 shows that the main environmental drivers of *E* were R_s and *D* in all seasons except for the wet season in 2016. For most seasons, *D* has a stronger effect than R_s on *E*. On these seasonal time scales, the influence of SWC, no matter which soil layer was considered, on *E* was weaker than that of

R_s and D.

Fig. 5 shows the specific relationships between environment variables (R_s·LAI and D·LAI) and E during the entire short rotation period. The relationships between E and R_s·LAI could generally be described by a strong linear relationship for each growing season, albeit with R^2 in 2016 (0.17-0.23) being much lower than that in other years (when R^2 ranged from 0.61 to 0.71) (Fig. 5a, c, e, and g). No relationship between E and D·LAI was found for 2016 (Fig. 5b). The relationships between E and D·LAI can be described by an exponential function from 2017 to 2019, with R^2 ranging from 0.78 to 0.88 (Fig. 5d, f, and h). These figures also show that E first increased rapidly when D·LAI increased, and then remained approximately constant after D reached a certain threshold (1.6 kPa (2017), 2 kPa (2018), 2.5 kPa (2019); these D values were converted from the D·LAI data in Fig. 5). For the same season, the relationships between E and environmental variables were similar among different water treatments.

From 8:00 am to 18:00 pm, for all treatments and using measured stomatal conductance for 2018, diurnal g_s, which varied from 60 to 800 mmol m^{-2} s^{-1} (Fig 6a), was regulated by D. The dependence of diurnal g_s on D could be described by a decreasing exponential function. Similarly, during the whole growing season, which run from mid-April to early September, g_{smax} decreased significantly when D increased; g_{smax} varied from 122 to 900 mmol m^{-2} s^{-1} (Fig 6b). We found no relationship with R_s, either g_s or g_{smax}. This was consistent with the fact that D was the main transpiration driver during the growing season. There was no difference in the functional relationships describing the regulation of stomata by D among different water treatments.

4. Discussion

4.1 Tree water use characteristics and its relationship with biomass production

Information on tree water use characteristics and their quantitative relationship with biomass production in a rotation is important for the establishment of biomass prediction models, and to establish a deep understanding of the mechanisms behind the relationship between tree water use and yield, under current and future climatic conditions. For poplar, many studies have reported its high water consumption characteristics, compared with other local tree species, which varied in the range of 320–700 mm $year^{-1}$ (Hinckley et al., 1994; Hall et al., 1996; Meiresonne et al., 1999; Bungart and Hüttl., 2004; Petzold et al., 2011). In our study, the annual water use of poplar during the full rotation period is

within this range, except for the 2-year-old (2016) stand of *P. tomentosa*, with an annual transpiration of around 200 mm, due to the relatively low LAI (with an annual maximum value of 2.5 m^2 m^{-2} (Li et al., 2020)).

The high water use of poplar leads to high biomass production in a short period of time, which is the main reason for the ongoing interest in commercial poplar plantations. Therefore, it is necessary to accurately evaluate the relationship between transpiration and biomass, as has been done in this study. Orság and Trnka (2011) and Fischer et al. (2014) revealed that there was a statistically significant linear relation between water use and biomass growth of hybrid poplar clone J-105 under environmental conditions representative of the Czech-Moravian Highlands. To our knowledge, no other reports on these kinds of relationships are available in the literatures. In our study, for each of the four years, the relationship between *E* and ABM increase of *P. tomentosa* followed a logistic relationship, with R^2 values of more than 0.89. No other reports on poplar water use studies mentioned such a relationship. The explanation for the fact that our findings diverge from those that reported linear relationships may be that they just explored the relationship before growth cessation (late August). However, for phenological reasons, the trees stop growing in autumn and hence the above-ground biomass accumulation stagnates, whereas the roots of the poplar trees are still actively absorbing soil water to meet the transpiration demand of existing leaves after vegetative growth cessation (Perry, 1971).

Thus, our first hypothesis, i.e., there is a strong linear relationship between transpiration and above-ground biomass, is rejected. Note that the shape of this relationship did not change for different water treatments and years. The logistic relationship between *E* and ABM implies that in autumn the trees are still consuming a lot of water, but there is no increase in yield. This is very important knowledge for seasonal irrigation management of poplar trees in the North China Plain. In addition, the relationship between total *E* and total ABM for the entire 5-year rotation period also follows a logistic relationship. This implies that the biomass increase will be very low in the years following 2019, which fits with the typical 5-year duration of *P. tomentosa* rotation with this planting density.

4.2 Biomass production under different water supply conditions

Understanding the effects of irrigation on tree biomass of different ages is crucial for decision-making on 'whether to irrigate' and 'how to irrigate' at the whole rotation scale. However, due to the lack of long-term near-continuous test data, it is difficult to accurately answer this question for *P. tomentosa* and many other poplar species. Some studies have shown that irrigation can significantly

improve the biomass yield of poplars (Liang et al., 2006; González-González et al. 2017; He et al., 2020). Also, Pairs et al. (2018) found that high amounts of irrigation water increased the biomass of 5- and 6-year-old (*P.* × *generosa*) × *P. nigra* by 31% and 79%, respectively. However, Hansen (1988) found that irrigation had no obvious effect on the growth of 5-year-old hybrid poplar trees, even though the annual biomass yield of 2- to 4-year-old poplar stands under high water supply conditions increased by 44%–76% compared with those under rainfed treatment. These results indicate that the effect of irrigation on biomass increase changed with tree age. In our study, the results showed that irrigation increased the biomass of *P. tomentosa* in each year of the rotation, leading to a total biomass increment of 59% (DIFI) and 46% (DICI), at the end of the rotation. This implies that irrigation is necessary in North China from the point of view of increasing biomass. However, trees still consume water at a rate similar to that observed in our study, which finding is important in the context of efficient irrigation management. When deciding whether to irrigate or how to irrigate, the focus should be on yield, because this determines the income for the farmers. However, the plantation water use, energy use and carbon footprint should also be included in the irrigation decision making process and subsequent irrigation scheduling. Otherwise, farmers might adopt wasteful energy and water use practices that increase biomass production at the expense of high energy inputs or high greenhouse gas emissions (Djomo et al., 2019). In this study, we only provide evidence that irrigation can increase the yield of poplar trees in short rotations in the North China Plain. However, in future studies, the economic benefits of water input and yield, and the environmental impacts should be taken into consideration to make efficient, resource-saving and environmentally friendly irrigation decisions.

4.3 Environment and plant controls of tree water use

R_s and D were the dominant variables driving transpiration, which has also been reported in Scots pine in Scotland (Wang et al., 2017), in balsam fir and black spruce (Oogathoo et al., 2020) in the humid boreal forest of eastern Canada, and in poplar trees in temperate China (Chen et al., 2014), for example. Likewise, in our multi-years study with a number of dry and wet seasons, E was strongly linearly related to R_s, which was consistent with the relationship between these variables described by Di et al. (2019b), also for *P. tomentosa*. However, Guan et al. (2012) reported that the relationship between E and R_s of *P. euramericana* was nonlinear. The variable responses of different poplar clones to environmental factors indicates that poplar species and their hybrids show a wide range of physiological mechanisms to control transpiration. The influence of D on E was different from that of R_s on E in our research. Other

researchers have described the relationship between D and E with exponential regressions (Guan et al., 2012; Chen et al., 2014) or linear regressions (Di et al., 2019b), for different poplar species. Our results show that E depends on D via an exponential function, that is, E and D are strongly linearly correlated when D is less than a certain threshold. Similar results have been reported for *P. tremuloides*: sap flow increased linearly with D, until D was about 1 kPa, but remained approximately constant after that (Hogg and Hurdle, 1997). Zhang et al. (1999) reported that the relationship between E and D reached an asymptote when $D > 1.2$ kPa for *P. trichocarpa*. Our results showed that the saturation point of D increased gradually with trees maturing, and changed from 1.6 kPa (2017) to 2.5 kPa (2019). This finding can probably be explained by the fact that as the trees mature, stronger, more extensive and deeper root networks can extract more water for transpiration to cope with atmospheric drought (Serra et al., 2014). For 2016, there was no significant relationship between E and D. This is possibly because 2-year-old young poplars have relatively low water requirements, and the soil water is sufficient to meet their transpiration consumption, so there is only a modest degree of atmospheric regulation of stomatal conductance.

Our results showed that SWC did not directly affect E, unlike R_s and D, even for the rainfed CK trees. Thus, our third hypothesis, that the main driver of E during dry seasons will shift from atmospheric variables (R_s and D) to soil water available, for water deficit conditions trees, is rejected. This indicates that differences in the amount of irrigation water applied to shallow soil do not directly affect the response of *P. tomentosa* transpiration to environmental factors. This is most likely due to the deep rooting characteristics of this species, so that it can extract water from deep soil layers, in the case of surface soil water deficit, to meet the high transpiration rate (Xi et al., 2018; Li et al., 2020). Chen et al. (2014), Di et al. (2018), Sun et al. (2018) and Yu et al. (2018) also reported that poplar roots can access deep soil water to alleviate water stress and help trees survive drought. Similarly, for other woody species, some studies also reported plants exploiting water reserves from deeper soil layers (David et al., 2004; Hernández-Santana et al., 2008; Thomas et al., 2006). In our study, for deep soil layers, we found that $SWC_{170\text{-}300}$ of the CK treatment was far lower than the equivalent SWC in the DIFI treatment in 2017 and 2019 (Fig 1g), which also supports this explanation. Moreover, the comparable responses of E to environmental variables among the different water treatments confirms this assumption. However, this finding is based on comparisons using daily SWC fluctuations, but the results may be different at coarser time scales.

Consistent with the high transpiration rates, g_s measured for *P. tomentosa* was generally high, with maximum values exceeding those of many other temperate tree species. In an extensive review of g_s measured in plants growing in natural conditions, Körner (1995) reported 0.19 ± 0.71 mol $m^{-2}s^{-1}$ as the mean maximum g_s of 22 temperate deciduous tree species. The maximum values we found for g_s (900 mmol $m^{-2}s^{-1}$, i.e., 0.9 mol m^{-2} s^{-1}) was much higher. However, high g_s values have also been observed in hybrid poplars in other studies. A maximum g_s of 760 mmol $m^{-2}s^{-1}$ was reported by Allen et al (1999) for *P. deltoides* × *P. nigra*. Moreover, other studies have shown that *D* fluctuation leads to variation in transpiration rate by affecting stomatal conductance (Franks et al., 2007; Meinzer et al., 1997; Renninger et al., 2010), and that a decline in stomatal conductance with increasing *D* indicates physiological restrictions to transpiration (Kučerová et al., 2010). Our results showed that in 2018, when *D* exceeded 2 kPa, g_{smax} was reduced to less than 200 mmol m^{-2} s^{-1}. These severely reduced values of g_s helped the canopy to avoid possible embolism caused by long-term atmospheric drought (Zhang et al., 1999). Thus, similar to other poplar clones, *P. tomentosa* also showed effective stomatal control on transpiration. The similar responses of g_s and g_{smax} to *D* among the different water treatments indicated that the relatively modest differences in shallow soil water status were not enough to change the physiological response process of *P. tomentosa*.

5. Conclusions

This study focused on the relationship between transpiration and biomass, as well as water use response to environmental variables, for *P. tomentosa* plantations in a whole short rotation period in the North China Plain. It also assessed the influence of different soil water conditions on the above relationships and response, including a rainfed treatment. We found that the aboveground biomass increase could be expressed as a function of accumulated *E*, through logistic curves (R^2 >0.89, P < 0.001), causing us to reject our first hypothesis. This finding is important for developing biomass prediction model and to improve our understanding of the mechanisms that shape the relationship between poplar water use and yield, in particular under changing environmental conditions. Our second hypothesis was upheld, i.e. that *E* was controlled by R_s and *D* for trees that were more than 2-years old (2017 onwards). *E* had a significant exponential relationship with *D*, which the maximum value of *D* that caused *E* to level off increased with tree age. Also, *E* had a significant linear relationship with R_s although with slightly weaker relationships than for *D*. Contrary to our third hypothesis, soil water

content did not become the dominant factor influencing E under water deficit conditions even for the rainfed treatment, and R_s and D remained the most important transpiration control variables. Our results have led to an improved understanding of the water-use strategies adopted by poplars in the North China Plain, and it will help to realize the sustainable management of poplar plantations in water-scarce regions around the world under changing environmental conditions.

Acknowledgements

This research was jointly supported by "National Natural Science Foundation of China" (32001304, 31872702, 31971640) and the National Key Research and Development Program of China (2016YFD0600403).

References

Allen, S. J., Hall, R. L., & Rosier, P. T., 1999. Transpiration by two poplar varieties grown as coppice for biomass production. Tree Physiol. 19(8), 493-501.

Bungart, R., & Hüttl, R. F., 2004. Growth dynamics and biomass accumulation of 8-year-old hybrid poplar clones in a short-rotation plantation on a clayey-sandy mining substrate with respect to plant nutrition and water budget. Eur J For Res. 123(2), 105-115.

Campbell, G. S., & Norman, J.M., 1998. An introduction to environmental biophysics. second ed. Springer, New York.

Chen, L., Zhang, Z., Zha, T., Mo, K., Zhang, Y., & Fang, X., 2014. Soil water affects transpiration response to rainfall and vapor pressure deficit in poplar plantation. New For (Dordr). 45(2), 235-250.

David, T. S., Ferreira, M. I., Cohen, S., Pereira, J. S., & David, J. S., 2004. Constraints on transpiration from an evergreen oak tree in southern Portugal. Agric For Meteorol. 122(3-4), 193-205.

Di, N., Liu, Y., Mead, D. J., Xie, Y., Jia, L., & Xi, B., 2018. Root-system characteristics of plantation-grown *Populus tomentosa* adapted to seasonal fluctuation in the groundwater table. Trees. 32(1), 137-149.

Di, N., Wang, Y., Clothier, B., Liu, Y., Jia, L., Xi, B., & Shi, H., 2019a. Modeling soil evaporation and the response of the crop coefficient to leaf area index in mature *Populus tomentosa* plantations growing under different soil water availabilities. Agric For Meteorol. 264, 125-137.

Di, N., Xi, B., Clothier, B., Wang, Y., Li, G., & Jia, L., 2019b. Diurnal and nocturnal transpiration behaviors and their responses to groundwater-table fluctuations and meteorological factors of *Populus tomentosa* in the North China Plain. For. Ecol. Manag. 448, 445-456.

Djomo, S. N., De Groote, T., Gobin, A., Ceulemans, R., & Janssens, I. A. 2019. Combining a land surface model with life cycle assessment for identifying the optimal management of short rotation coppice in Belgium. Biomass Bioenergy. 121, 78-88.

FAO International poplar commission, 2016. Poplars and Other Fast-Growing Trees - Renewable Resources for Future Green Economies. http://www.fao.org/forestry/ipc2016/en/.

Fischer, M., Trnka, M., Kučera, J., Fajman, M., & Žalud, Z., 2014. Biomass productivity and water use relation in short rotation poplar coppice (*Populus nigra x P. maximowiczii*) in the conditions of Czech Moravian Highlands. Acta Univ. Agric. et Silvic. Mendelianae Brun. *59*(6), 141-152.

Franks, P. J., Drake, P. L., & Froend, R. H. (2007). Anisohydric but isohydrodynamic: seasonally constant plant water potential gradient explained by a stomatal control mechanism incorporating variable plant hydraulic conductance. Plant Cell Environ. 30(1), 19-30.

González-González, B. D., Oliveira, N., González, I., Cañellas, I., & Sixto, H., 2017. Poplar biomass production in short rotation under irrigation: A case study in the Mediterranean. Biomass and Bioenergy. 107, 198-206.

Grömping, U., 2006. Relative importance for linear regression in R: the package relaimpo. J. Stat. Softw. 17(1), 1-27.

Granier, A., 1987. Evaluation of transpiration in a Douglas fir stand by means of sap flow measurements. Tree Physiol. 3 (4), 309–320.

Guan, D. X., Zhang, X. J., Yuan, F. H., Chen, N. N., Wang, A. Z., Wu, J. B., & Jin, C. J., 2012. The relationship between sap flow of intercropped young poplar trees (*Populus*× *euramericana* cv. N3016) and environmental factors in a semiarid region of northeastern China. J. Stat. Softw. 26(19), 2925-2937.

Hall, R. L., Allen, S. J., Rosier, P. T. W., Smith, D. M., Hodnett, M. G., Roberts, J. M., ... & Gooddy, D. C., 1996. Hydrological effects of short rotation energy coppice. Final report to ETSU.

Hamanishi, E. T., Raj, S., Wilkins, O., Thomas, B. R., Mansfield, S. D., Plant, A. L., & Campbell, M. M., 2010. Intraspecific variation in the *Populus balsamifera* drought transcriptome. Plant Cell Environ. 33(10), 1742-1755.

Hansen, E.A., 1988. Irrigating short rotation intensive culture hybrid poplars. Biomass, 16, 237–250.

He, Y., Xi, B., Bloomberg, M., Jia, L., & Zhao, D., 2020. Effects of drip irrigation and nitrogen fertigation on stand growth and biomass allocation in young triploid *Populus tomentosa* plantations. For. Ecol. Manag. 461, 117937.

Hernández-Santana, V., David, T. S., & Martínez-Fernández, J., 2008. Environmental and plant-based controls of water use in a Mediterranean oak stand. For. Ecol. Manag. 255(11), 3707-3715.

Hernandez-Santana, V., Fernández, J. E., Rodriguez-Dominguez, C. M., Romero, R., & Diaz-Espejo, A., 2016. The dynamics of radial sap flux density reflects changes in stomatal conductance in response to soil and air water deficit. Agric For Meteorol. 218, 92-101.

Hinckley, T. M., Brooks, J. R., Čermák, J., Ceulemans, R., Kučera, J., Meinzer, F. C., & Roberts, D. A., 1994. Water flux in a hybrid poplar stand. Tree Physiol. 14(7-8-9), 1005-1018.

Hogg, E. H., & Hurdle, P. A., 1997. Sap flow in trembling aspen: implications for stomatal responses to vapor pressure deficit. Tree Physiol. 17(8-9), 501-509.

Kang, S., & Eltahir, E. A., 2018. North China Plain threatened by deadly heatwaves due to climate change and irrigation. Nat. Commun. 9(1), 1-9.

Körner, C., 1995. Leaf diffusive conductances in the major vegetation types of the globe. In Ecophysiology of photosynthesis (pp. 463-490). Springer, Berlin, Heidelberg.

Kučerová, A., Čermák, J., Nadezhdina, N., & Pokorný, J., 2010. Transpiration of *Pinus rotundata* on a wooded peat bog in central Europe. Trees. 24(5), 919-930.

Larchevêque, M., Maurel, M., Desrochers, A., & Larocque, G. R., 2011. How does drought tolerance compare between two improved hybrids of balsam poplar and an unimproved native species?. Tree Physiol. 31(3), 240-249.

Li, D., Fernández, J. E., Li, X., Xi, B., Jia, L., & Hernandez-Santana, V., 2020. Tree growth patterns and diagnosis of water status based on trunk diameter fluctuations in fast-growing *Populus tomentosa* plantations. Agric Water Manag. 241, 106348.

Liang, Z. S., Yang, J. W., Shao, H. B., & Han, R. L., 2006. Investigation on water consumption characteristics and water use efficiency of poplar under soil water deficits on the Loess Plateau. Colloids Surf. B. 53(1), 23-28.

Meiresonne, L., Nadezhdin, N., Cermak, J., Van Slycken, J., & Ceulemans, R., 1999. Measured sap flow and simulated transpiration from a poplar stand in Flanders (Belgium). Agric For Meteorol. 96, 165-179.

Meinzer, F. C., Hinckley, T. M., & Ceulemans, R., 1997. Apparent responses of stomata to transpiration and humidity in a hybrid poplar canopy. Plant Cell Environ. 20(10), 1301-1308.

Oogathoo, S., Houle, D., Duchesne, L., & Kneeshaw, D., 2020. Vapour pressure deficit and solar radiation are the major drivers of transpiration of balsam fir and black spruce tree species in humid boreal regions, even during a short-term drought. Agric For Meteorol, 291, 108063.

Orság, M., & Trnka, M., 2011. Transpiration and biomass increment in short rotation poplar coppice. In Proceedings of International PhD Students Conference “MendelNet”. Brno (Czech Republic) 2011 (pp. 688-693).

Paris, P., Matteo, G.D., Tarchi, M., Tosi, L., Spaccino, L., 2018. Precision subsurface drip irrigation increases yield while sustaining water-use efficiency in Mediterranean poplar bioenergy

plantations. For. Ecol. Manag. 409, 749–756.

Perry, T. O., 1971. Dormancy of trees in winter. Science. 171(3966), 29-36.

Petzold, R., Schwärzel, K., & Feger, K. H., 2011. Transpiration of a hybrid poplar plantation in Saxony (Germany) in response to climate and soil conditions. Eur J For Res. 130(5), 695-706.

Renninger, H. J., Phillips, N., & Salvucci, G. D., 2010. Wet - vs. dry - season transpiration in an Amazonian rain forest palm Iriartea deltoidea. Biotropica. 42(4), 470-478.

Serra, I., Strever, A., Myburgh, P. A., & Deloire, A., 2014. the interaction between rootstocks and cultivars (*Vitis vinifera* L.) to enhance drought tolerance in grapevine. Aust. J. Grape Wine Res. 20(1), 1-14.

Sun, S., He, C., Qiu, L., Li, C., Zhang, J., & Meng, P., 2018. Stable isotope analysis reveals prolonged drought stress in poplar plantation mortality of the Three-North Shelter Forest in Northern China. Agric For Meteorol. 252, 39-48.

Thomas, F. M., Foetzki, A., Arndt, S. K., Bruelheide, H., Gries, D., Li, X., ... & Runge, M., 2006. Water use by perennial plants in the transition zone between river oasis and desert in NW China. Basic Appl Ecol. 7(3), 253-267.

Tie, Q., Hu, H., Tian, F., Guan, H., & Lin, H., 2017. Environmental and physiological controls on sap flow in a subhumid mountainous catchment in North China. Agric For Meteorol. 240, 46-57.

Tognetti, R., Giovannelli, A., Lavini, A., Morelli, G., Fragnito, F., & d'Andria, R., 2009. Assessing environmental controls over conductances through the soil–plant–atmosphere continuum in an experimental olive tree plantation of southern Italy. Agric For Meteorol. 149(8), 1229-1243.

Wang, H., Tetzlaff, D., Dick, J. J., & Soulsby, C., 2017. Assessing the environmental controls on Scots pine transpiration and the implications for water partitioning in a boreal headwater catchment. Agric For Meteorol. 240, 58-66.

Xi, B.Y., 2013. Research on Theories of Irrigation Management and Key Techniques of High Efficient Subsurface Drip Irrigation in *Populus tomentosa* Plantation. Beijing Forestry University, Beijing, China (in Chinese).

Xi, B.Y., Bloomberg, M., Watt, M.S., Wang, Y., Jia, L.M., 2016. Modeling growth response to soil water availability simulated by HYDRUS for a mature triploid *Populus tomentosa* plantation located on the North China Plain. Agric. Water Manag. 176, 243–254.

Xi, B., Di, N., Cao, Z., Liu, J., Li, D., Wang, Y., Li, G., Duan, J., Jia, L., Zhang, R., 2018. Characteristics

and underlying mechanisms of plant deep soil water uptake and utilization: implication for the cultivation of plantation trees. Chinese J. Plant Ecol. 42, 885–905 in Chinese with English abstract.

Yu, T., Feng, Q., Si, J., Mitchell, P. J., Forster, M. A., Zhang, X., & Zhao, C. 2018. Depressed hydraulic redistribution of roots more by stem refilling than by nocturnal transpiration for *Populus euphratica* Oliv. in situ measurement. Ecol Evol. 8(5), 2607-2616.

Zhang, H., Morison, J. I., & Simmonds, L. P., 1999. Transpiration and water relations of poplar trees growing close to the water table. Tree Physiol. 19(9), 563-573.

Zhang, P.D., Wu, F., Kang, X.Y., 2012. Genotypic variation in wood properties and growth traits of triploid hybrid clones of *Populus tomentosa* at three clonal traits. Tree Genet. Genomes. 8 (5), 1041–1050.

Figure

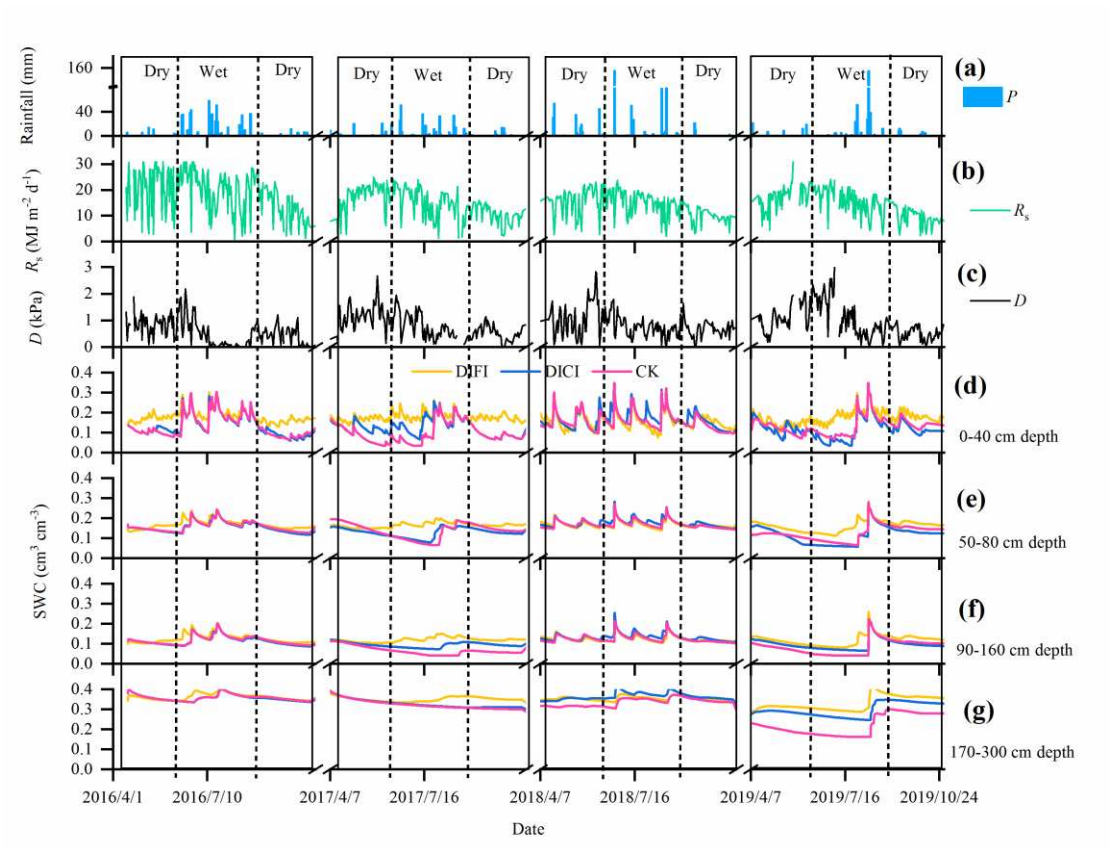

Fig. 1 Environmental variables during the growing seasons from 2016 to 2019. (a) Daily total precipitation (P), (b) solar radiation (R_s), (c) daily average vapor pressure deficit (D), and (d-g) daily average soil water content (SWC) at different soil depths. The divide between the dry and wet seasons has been set to occur in mid-June and late August as indicated by the dotted vertical line.

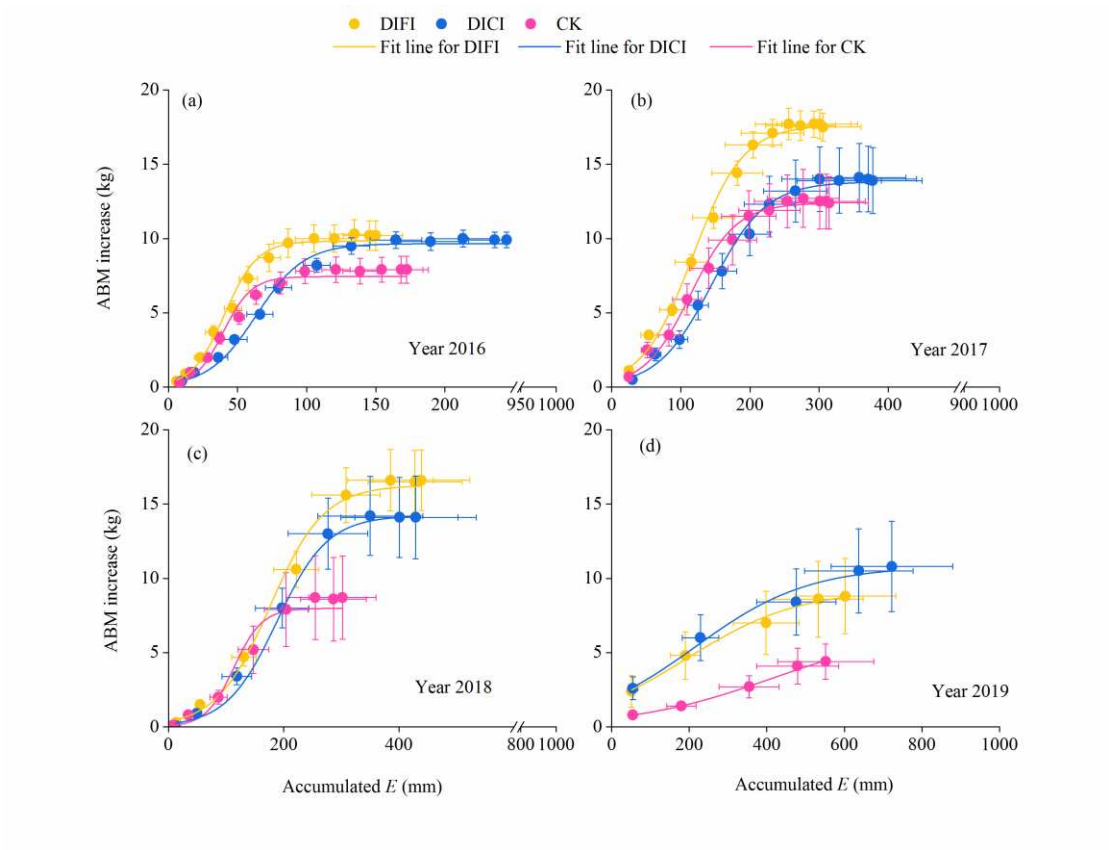

Fig. 2 Relationship between accumulated transpiration (*E*) and aboveground biomass (ABM) increase throughout the entire short rotation period: (a) 2016, (b) 2017, (c) 2018 and (d) 2019 under drip full irrigation (DIFI), drip control irrigation (DICI) and non-irrigation (CK) treatments. Each point is based on the average ABM increase and accumulated *E* of 5 trees per treatment. The calculation of accumulated *E* started on the first day that ABM was calculated, for each growing season, and ended in October. Error bars represent standard errors.

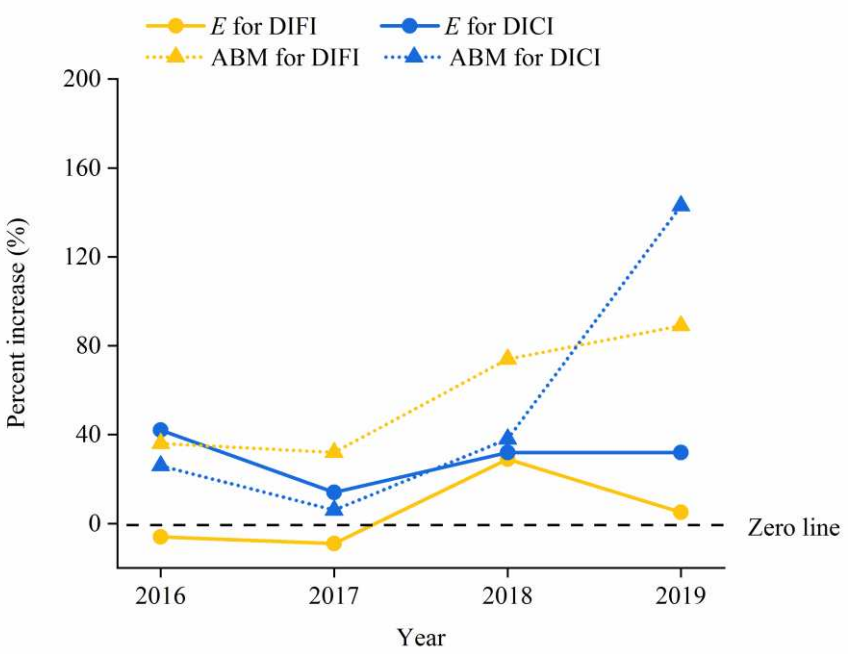

Fig. 3 The percent increase (PI) of aboveground biomass (ABM) and transpiration (*E*) in drip full irrigation (DIFI) and drip control irrigation (DICI) compared with the non-irrigation treatment (CK), for each year. Each point represents the percentage increase of the annual increase in *E* or biomass of trees under DIFI and DICI compared to those of the CK. For example: $PI_{E\text{-DIFI}} = ((E_{DIFI} - E_{CK})/ E_{CK}) \times 100$. The *E* and ABM of each tree were normalized by dividing them by the initial diameter at breast height (DBH) to eliminate the effect of initial tree size on the results. The black dotted line represents the zero PI line.

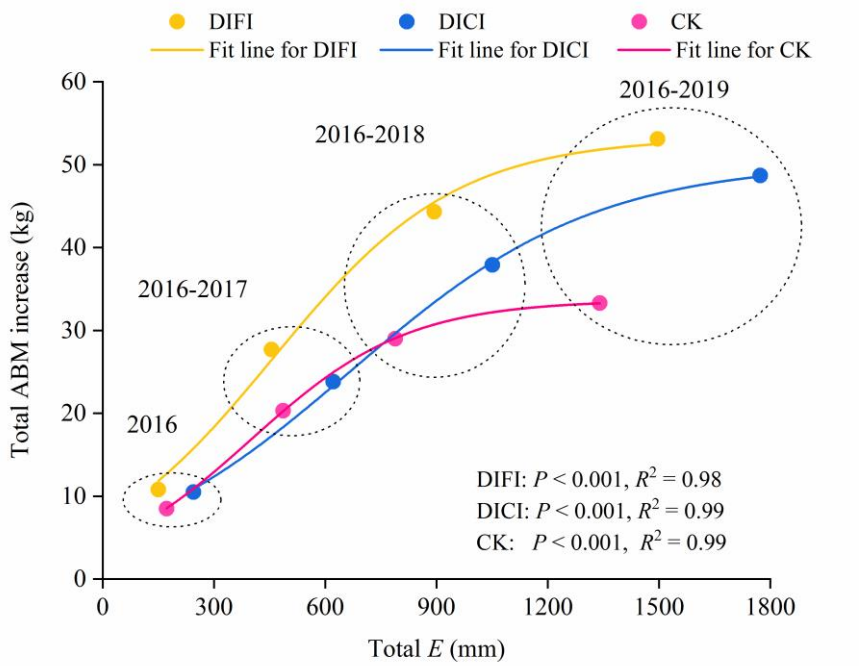

Fig. 4 Relationship between total accumulated transpiration (*E*) and aboveground biomass (ABM) increase at the end of each growing season, for the entire rotation period, under drip full irrigation (DIFI), drip control irrigation (DICI) and non-irrigtion (CK) treatments. Each point is based on the average ABM increase and accumulated *E* of 5 trees per treatment. The calculation of accumulated *E* started on the first day that ABM was calculated, for each growing season, and ended in October. The *E* and ABM of each treatment were normalized by dividing them by the initial diameter at breast height (DBH) to eliminate the effect of initial tree size on the results. Each dotted circle represents the three treatments at the end of the same growing season.

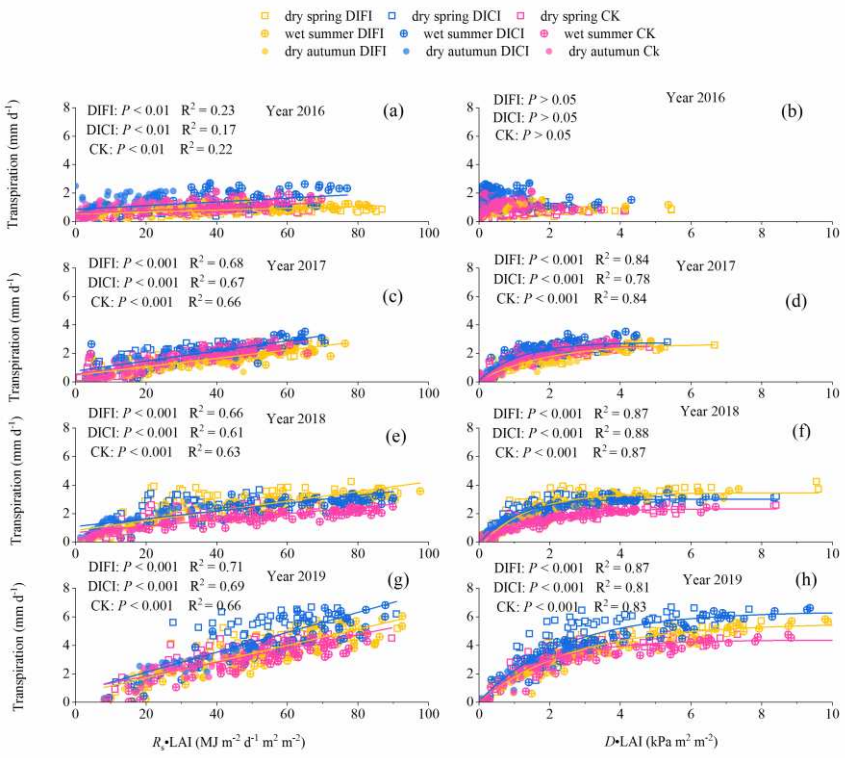

Fig. 5 Relationships between transpiration and some environmental variables from 2016 to 2019. D, R_s and LAI indicate vapor pressure deficit, solar radiation and leaf area index, respectively.

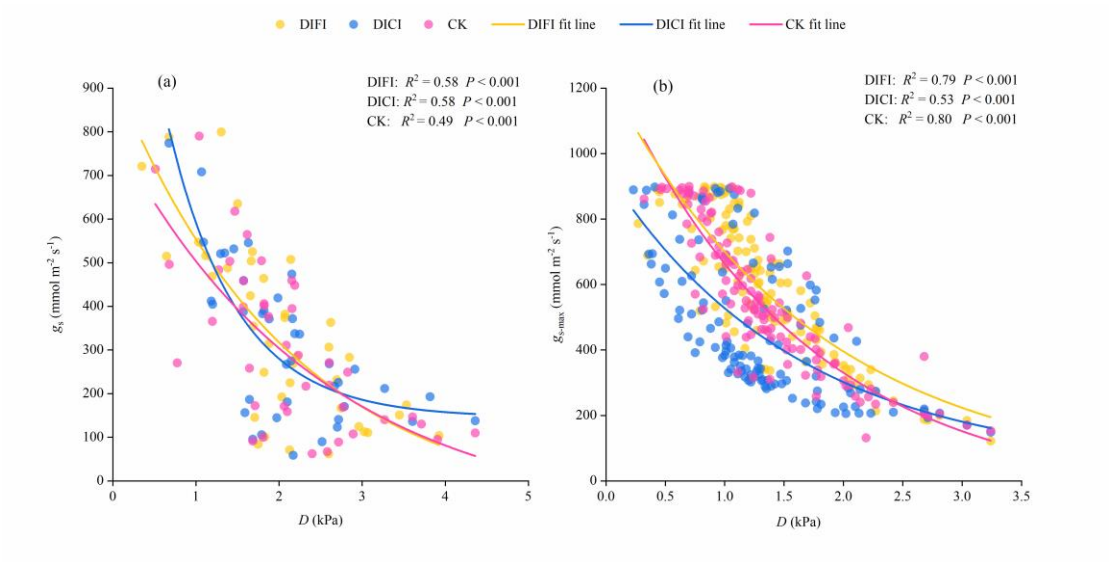

Fig. 6 (a) Relationship between stomatal conductance (g_s) measured with a porometer and vapor pressure deficit (D). Each point represents the average of three leaves in one tree per treatment. Monitoring of g_s took place for each half hour during 8:00 am to 18:00 pm on six sunny days (April 15th, April 18th, April 25th, May 13th, May 23th and June 20th). (b) Relationship between modelled g_{smax} and D from April to late August in 2018. Each point represents the g_{smax} of a typical sunny day of the tree which was monitored for modeled g_s.

Declaration of interests

☒ The authors declare that they have no known competing financial interests or personal relationships that could have appeared to influence the work reported in this paper.

☐The authors declare the following financial interests/personal relationships which may be considered as potential competing interests: